Available online at www.sciencedirect.com
SCIENCE DIRECT
Journal of Sound and Vibration 297 (2006) 146–166
JOURNAL OF SOUND AND VIBRATION
www.elsevier.com/locate/jsvi

Free vibration of rectangular plates with internal column supports

Ding Zhou[a,b,*], Tianjian Ji[b]

[a]College of Civil Engineering, Nanjing University of Technology, Nanjing 210009, People's Republic of China
[b]School of Mechanical, Aerospace and Civil Engineering, The University of Manchester, Manchester, UK

Received 8 March 2005; received in revised form 15 March 2006; accepted 16 March 2006
Available online 2 June 2006

Abstract

A direct method is proposed to derive the exact solution for the free vibration of a thin rectangular plate with two opposite edges simply supported and with internal column supports. Considering the compatibility of displacements and rotations between the plate and the columns, the coupled vibration of a plate–column system is derived. The accuracy and correctness of the present method are demonstrated through the comparison of the results obtained from the proposed method and from finite-element analysis. Then the effects of column sizes and column models on the natural frequencies of a plate–column system are investigated in detail. A parametric study is focused on fully simply supported rectangular plates with a single internal column. It is shown that the effect of column flexibility in plate–column structures should be considered. The solution provided in the paper is general and includes several particular solutions for fixed point-supports, pinned point-supports and elastic point-supports. Results with high accuracy have been obtained and these can be used as the benchmark for the further investigation and for other approximate methods.

1. Introduction

Floor slabs supported by columns are typical structures in civil engineering. For a long-span flat slab, the internal column supports can greatly enhance the loading capacity and improve the dynamic characteristics of the slab. Therefore, it is important for designers to understand how the columns affect the dynamic characteristics of a floor structure [1].

There are several models to describe the effect of a column on the vibration of a floor. The simplest model is to consider the column as having infinite stiffness in the longitudinal direction, i.e., a pinned point-support. An improved model is to consider the effect of the stiffness of the column, i.e., to model the column as three massless springs in the longitudinal and two rotational directions.

There are many publications on free vibration of plates with either rigid or elastic point-supports and only a typical selection is mentioned here. A general study to vibration characteristics of rectangular plates with arbitrarily located point-supports came from Fan and Cheung [2] using the spline finite strip method. Kim and

*Corresponding author. College of Civil Engineering, Nanjing University of Technology, Nanjing 210009, People's Republic of China. Tel.: +86 25 84316695.
E-mail address: dingzhou57@yahoo.com (D. Zhou).

0022-460X/$ - see front matter © 2006 Elsevier Ltd. All rights reserved.
doi:10.1016/j.jsv.2006.03.031

Dickinson [3] used the Lagrangian multiplier method combined with the orthogonally generated polynomials to study the rectangular plates with point-supports. Zhou [4] and Cheung and Zhou [5] used static beam functions as admissible functions to study tapered rectangular plates with point-supports and composite rectangular plates with point-supports, respectively. The 3-D vibration of composite plates with internal point-supports has been studied by Zhou et al. [6] using the finite layer method. Liew et al. [7] studied the free vibration of arbitrarily shaped Mindlin plates with internal point-supports. Bergman et al. [8] derived the dynamic Green function for rectangular plates having two opposite edges simply supported and attached by substructures. Petyt and Mirza [9] used the finite-element (FE) method to study the free vibration of column-supported floor slabs by simplifying the columns as pinned point-supports. El-Dardiry et al. [10] examined the effects of FE models on the dynamic characteristics of a column-supported long-span flat concrete floor. Three different models for the columns: pinned point-supports, fixed point-supports and continuous columns, were considered. The predicted frequencies of the three models were compared with 11 measured natural frequencies of the floor. This showed that the column-floor model provided the most appropriate representation of the floor system. The results also indicated that the first 12 calculated natural frequencies of the column-floor model were just between the corresponding natural frequencies of the pinned point-support and fixed point-support models [10]. This paper will show that this observation cannot be used as a general conclusion.

In the present study, the exact analytical solution for a thin rectangular plate with two opposite edges simply supported and with internal column supports is derived directly from the governing differential equations. The eigenvalue equations are then obtained by considering the compatibility of displacements and rotations between the plate and the columns. The number of the eigenvalue equations equals to three times of the number of the columns. The natural frequencies are determined by using the searching root method. Several special cases can be directly derived from the solutions. The correctness and accuracy of the proposed method is first verified by using the FE method, then parametric studies are conducted to examine the effects of the ratio of the dimensions of plate to column, the ratio of the diameter of column to the thickness of a plate and different column models.

2. Governing differential equations

A uniform thin rectangular plate with n internal column supports is considered as shown in Fig. 1. It is assumed that the plate is simply supported at two opposite edges $x = 0$ and $x = a$, and the length and width of the plate are a and b, respectively. According to the theory of thin plate vibration, the governing differential equation is given as follows:

$$D\left(\frac{\partial^4 w}{\partial x^4} + 2\frac{\partial^4 w}{\partial x^2 \partial y^2} + \frac{\partial^4 w}{\partial y^4}\right) + C_p \frac{\partial w}{\partial t} + \rho h \frac{\partial^2 w}{\partial t^2} = f(x, y, t) + f_0(x, y, t), \tag{1}$$

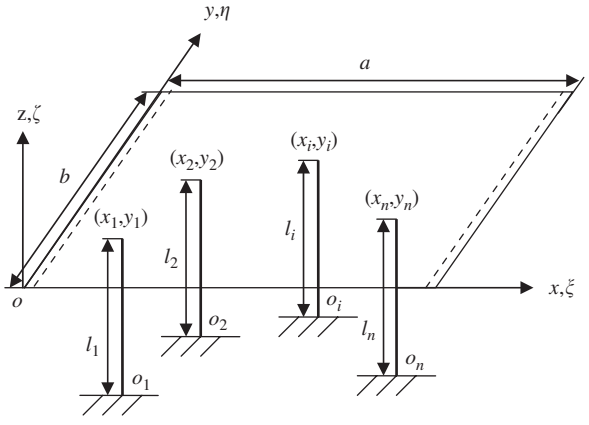

Fig. 1. A rectangular plate with internal column supports.

where w is the transverse deflection of the plate, ρ is the mass density per unit volume, h is the thickness of the plate, D is the flexural rigidity and C_p is the damping of the plate. $f_0(x, y, t)$ and $f(x, y, t)$ are the external loads acting on the plate and the forces between the internal columns and the plate. The internal forces can be expressed as:

$$f(x,y,t) = \sum_{i=1}^{n} p_i(t)\delta(x-x_i)\delta(y-y_i) + \sum_{i=1}^{n} m_{xi}(t)\delta'(x-x_i)\delta(y-y_i) + \sum_{i=1}^{n} m_{yi}(t)\delta(x-x_i)\delta'(y-y_i), \tag{2}$$

where $p_i(t)$ is the vertical internal force of the ith column acting on the plate, $m_{xi}(t)$ and $m_{yi}(t)$ are the bending moments, respectively, about the y and x axes, (x_i, y_i) is the position of the ith column, $\delta(x-x_i)$ and $\delta(y-y_i)$ are the Dirac delta functions, and $\delta'(x-x_i)$ and $\delta'(y-y_i)$ are the doublet functions.

Assuming that the principal axes of the cross-section of all columns are parallel to the x and y axes, the transverse vibration of the ith column should satisfy the following two governing differential equations

$$E_i I_{xi}\frac{\partial^4 v_{xi}}{\partial z^4} + C_{vi}\frac{\partial v_{xi}}{\partial t} + \rho_i A_i \frac{\partial^2 v_{xi}}{\partial t^2} = q_{xi}(z,t), \quad i = 1,2,\ldots,n, \tag{3}$$

$$E_i I_{yi}\frac{\partial^4 v_{yi}}{\partial z^4} + C_{vi}\frac{\partial v_{yi}}{\partial t} + \rho_i A_i \frac{\partial^2 v_{yi}}{\partial t^2} = q_{yi}(z,t), \quad i = 1,2,\ldots,n, \tag{4}$$

where E_i is the modulus of elasticity of the ith column, I_{xi} and I_{yi} are the second moments of area of the ith column in the $o_i xz$ and $o_i yz$ planes respectively, and v_{xi} and v_{yi} are the deflections in the x and y directions, respectively, C_{vi} is the damping for the transverse vibration of the ith column and $\rho_i A_i$ is the mass density per unit length. $q_{xi}(z, t)$ and $q_{yi}(z, t)$ are the external forces acting on the ith column within the $o_i xz$ and $o_i yz$ planes, respectively.

The longitudinal vibration of the ith column should satisfy the following governing differential equation:

$$-E_i A_i \frac{\partial^2 u_i}{\partial z^2} + C_{ui}\frac{\partial u_i}{\partial t} + \rho_i A_i \frac{\partial^2 u_i}{\partial t^2} = f_i(z,t), \quad i = 1,2,\ldots,n, \tag{5}$$

where u_i is the displacement of the ith column in the longitudinal direction, C_{ui} is the damping coefficient for the longitudinal vibration of the ith column and $f_i(z, t)$ is the external load in the longitudinal direction.

When the plate–column system experiences free vibration, $f_0(x, y, t) = 0$, $q_{xi}(z, t) = 0$, $q_{yi}(z, t) = 0$ and $f_i(z, t) = 0$, $(i = 1, 2, \ldots, n)$. The solutions of Eqs. (1)–(5) have the following forms when the damping effect is neglected:

$$\begin{aligned} &w = W(x,y)e^{j\omega t}, \quad f(x,y,t) = F(x,y)e^{j\omega t}, \quad p_i(t) = P_i e^{j\omega t},\\ &m_{xi}(t) = M_{xi}e^{j\omega t}, \quad m_{yi}(t) = M_{yi}e^{j\omega t}, \quad v_{xi}(z,t) = V_{xi}(z)e^{j\omega t},\\ &v_{yi}(z,t) = V_{yi}(z)e^{j\omega t}, \quad u_i(z,t) = U_i(z)e^{j\omega t}, \end{aligned} \tag{6}$$

where $W(x, y)$, $V_{xi}(z)$, $V_{yi}(z)$ and $U_i(z)$ are the displacement functions. $F(x, y)$ and P_i are the amplitudes of forces. M_{xi} and M_{yi} are the amplitudes of bending moments. ω is the natural frequency of the plate–column system and $j = \sqrt{-1}$.

Using the following dimensionless coordinates

$$\xi = x/a, \quad \eta = y/b, \quad \zeta_i = z/l_i, \quad \xi_i = x_i/a, \quad \eta_i = y_i/b \tag{7}$$

and substituting Eqs. (6) and (7) into Eqs. (1)–(5) leads to

$$\frac{1}{\beta^4}\frac{\partial^4 W}{\partial \xi^4} + \frac{2}{\beta^2}\frac{\partial^4 W}{\partial \xi^2 \partial \eta^2} + \frac{\partial^4 W}{\partial \eta^4} - \frac{\rho h}{D} b^4 \omega^2 W = \frac{b^4}{D} F(\xi,\eta), \tag{8}$$

$$F(\xi,\eta)=\frac{1}{ab}\sum_{i=1}^{n}P_i\delta(\xi-\xi_i)\delta(\eta-\eta_i)+\frac{1}{a^2b}\sum_{i=1}^{n}M_{xi}\delta'(\xi-\xi_i)\delta(\eta-\eta_i)+\frac{1}{ab^2}\sum_{i=1}^{n}M_{yi}\delta(\xi-\xi_i)\delta'(\eta-\eta_i), \tag{9}$$

$$\frac{\mathrm{d}^4V_{xi}}{\mathrm{d}\zeta_i^4}-\frac{\rho_iA_i}{E_iI_{xi}}l_i^4\omega^2V_{xi}=0,\quad \frac{\mathrm{d}^4V_{yi}}{\mathrm{d}\zeta_i^4}-\frac{\rho_iA_i}{E_iI_{yi}}l_i^4\omega^2V_{yi}=0, \tag{10}$$

$$\frac{\mathrm{d}^2U_i}{\mathrm{d}\zeta_i^2}+\frac{\rho_i}{E_i}l_i^2\omega^2U_i=0, \tag{11}$$

where $\beta=a/b$ is the aspect ratio of the plate. Eqs. (8)–(11) are the governing equations of free vibration for the plate–column system.

3. Boundary and compatibility conditions

Considering that the plate is elastically restrained at the edges $\eta=0$ and 1, its boundary conditions are given by

$$\frac{\partial^2W}{\partial\eta^2}+v\frac{\partial^2W}{\beta^2\partial\xi^2}=\frac{bk_{r0}}{D}\frac{\partial W}{\partial\eta},\quad \text{at } \eta=0, \tag{12a}$$

$$\frac{\partial^2W}{\partial\eta^2}+v\frac{\partial^2W}{\beta^2\partial\xi^2}=-\frac{bk_{rb}}{D}\frac{\partial W}{\partial\eta},\quad \text{at } \eta=1, \tag{12b}$$

$$\frac{\partial^3W}{\partial\eta^3}+(2-v)\frac{\partial^3W}{\beta^2\partial\eta\partial\xi^2}=-\frac{b^3k_{t0}}{D}W,\quad \text{at } \eta=0, \tag{12c}$$

$$\frac{\partial^3W}{\partial\eta^3}+(2-v)\frac{\partial^3W}{\beta^2\partial\eta\partial\xi^2}=\frac{b^3k_{tb}}{D}W,\quad \text{at } \eta=1, \tag{12d}$$

where k_{r0} and k_{rb} are the stiffnesses of the rotational restraints at boundaries $\eta=0$ and $\eta=1$ respectively, k_{t0} and k_{tb} are the stiffnesses of the vertical restraints at $\eta=0$ and $\eta=1$ respectively. By taking these stiffness coefficients to be infinite or zero, various classical boundary conditions of the plate can be obtained.

- $k_{r0}=k_{rb}=0$ and $k_{t0}=k_{tb}=\infty$, the plate is simply supported at $\eta=0$ and $\eta=1$.
- $k_{r0}=k_{rb}=\infty$ and $k_{t0}=k_{tb}=\infty$, the plate is clamped at $\eta=0$ and $\eta=1$.
- $k_{r0}=k_{rb}=0$ and $k_{t0}=k_{tb}=0$, the plate is free at $\eta=0$ and $\eta=1$.

Similarly, general boundary conditions can also be considered for the columns. For the ith column:

$$\frac{\mathrm{d}^2V_{xi}}{\mathrm{d}^2\zeta_i}=\frac{k_{xri}l_i}{E_iI_{xi}}\frac{\mathrm{d}V_{xi}}{\mathrm{d}\zeta_i},\quad \frac{\mathrm{d}^3V_{xi}}{\mathrm{d}\zeta_i^3}=-\frac{k_{xti}l_i^3}{E_iI_{xi}}V_{xi}\quad \text{at } \zeta_i=0, \tag{13a}$$

$$V_{xi}=0,\quad \frac{\mathrm{d}^2V_{xi}}{\mathrm{d}^2\zeta_i}=\frac{M_{xi}l_i^2}{E_iI_{xi}}\quad \text{at } \zeta_i=1, \tag{13b}$$

$$\frac{\mathrm{d}^2V_{yi}}{\mathrm{d}^2\zeta_i}=\frac{k_{yri}l_i}{E_iI_{yi}}\frac{\mathrm{d}V_{yi}}{\mathrm{d}\zeta_i},\quad \frac{\mathrm{d}^3V_{yi}}{\mathrm{d}\zeta_i^3}=-\frac{k_{yti}l_i^3}{E_iI_{yi}}V_{yi}\quad \text{at } \zeta_i=0, \tag{13c}$$

$$V_{yi} = 0, \quad \frac{\mathrm{d}^2 V_{yi}}{\mathrm{d}\zeta_i^2} = \frac{M_{yi} l_i^2}{E_i I_{yi}} \quad \text{at } \zeta_i = 1, \tag{13d}$$

$$\frac{\mathrm{d}U_i}{\mathrm{d}\zeta_i} = \frac{k_{zi} l_i}{E_i A_i} U_i \quad \text{at } \zeta_i = 0, \tag{13e}$$

$$\frac{\mathrm{d}U_i}{\mathrm{d}\zeta_i} = \frac{P_i l_i}{E_i A_i} \quad \text{at } \zeta_i = 1, \tag{13f}$$

where k_{xri} and k_{xti} are, respectively, the stiffnesses of the rotational and translational restraints of the ith column in the $o_i xz$ plane at the end $\zeta_i = 0$. k_{yri} and k_{yti} are the equivalent in the $o_i yz$ plane at the end $\zeta_i = 0$. k_{zi} is the stiffness of the longitudinal constraint of the ith column at the end $\zeta_i = 0$. By taking these stiffness coefficients to be infinite or zero, several classical boundary conditions of the column can be obtained.

- $k_{xri} = k_{yri} = 0$, $k_{xti} = k_{yti} = \infty$ and $k_{zi} = \infty$, the ith column is simply supported at $\zeta_i = 0$.
- $k_{xri} = k_{yri} = \infty$, $k_{xti} = k_{yti} = \infty$ and $k_{zi} = \infty$, the ith column is clamped at $\zeta_i = 0$.

The compatibility conditions of displacements and rotations between the plate and the columns are respectively:

$$W(\xi, \eta)\big|_{\xi=\xi_i, \eta=\eta_i} = -U_i(\zeta_i)\big|_{\zeta_i=1}, \tag{14a}$$

$$\left.\frac{\partial W}{\partial \xi}\right|_{\xi=\xi_i, \eta=\eta_i} = -\frac{a}{l_i}\left.\frac{\partial V_{xi}}{\partial \zeta_i}\right|_{\zeta_i=1}, \quad \left.\frac{\partial W}{\partial \eta}\right|_{\xi=\xi_i, \eta=\eta_i} = -\frac{b}{l_i}\left.\frac{\partial V_{yi}}{\partial \zeta_i}\right|_{\zeta_i=1}, \quad i = 1, 2, \ldots, n. \tag{14b}$$

4. Solutions

For a plate with two opposite edges simply supported, its solution can be given as

$$W(\xi, \eta) = \sum_{m=1}^{\infty} \sin(m\pi\xi) W_m(\eta). \tag{15}$$

It is clear that the above equation exactly satisfies the simply supported conditions at edges $\xi = 0$ and $\xi = 1$.

Now, expanding $F(\xi, \eta)$ into a Fourier sinusoidal series as follows

$$F(\xi, \eta) = 2\sum_{m=1}^{\infty} \sin(m\pi\xi) F_m(\eta), \quad F_m(\eta) = \int_0^1 F(\xi, \eta) \sin(m\pi\xi)\, \mathrm{d}\xi \tag{16}$$

and substituting Eqs. (15) and (16) into Eq. (8) leads to:

$$\frac{\mathrm{d}^4 W_m(\eta)}{\mathrm{d}\eta^4} - 2\frac{(m\pi)^2}{\beta^2}\frac{\mathrm{d}^2 W_m(\eta)}{\mathrm{d}\eta^2} + \left[\frac{(m\pi)^4}{\beta^4} - \alpha^4\right] W_m(\eta) = 2\frac{b^4}{D} F_m(\eta), \tag{17}$$

where $\alpha^4 = \rho h b^4 \omega^2 / D$. The solution of Eq. (17) can be obtained using the theory of ordinary differential equation.

When $\alpha < m\pi/\beta$:

$$W_m(\eta) = A_m \sinh(\lambda_{m1}\eta) + B_m \cosh(\lambda_{m1}\eta) + C_m \sinh(\lambda_{m2}\eta) + D_m \cosh(\lambda_{m2}\eta) + \tilde{W}_m(\eta), \tag{18a}$$

$$\tilde{W}_m(\eta) = \frac{b^4}{D\alpha^2 \lambda_{m1}\lambda_{m2}} \int_0^{\eta} F_m(s)[\lambda_{m1} \sinh(\lambda_{m2}(\eta - s)) - \lambda_{m2} \sinh(\lambda_{m1}(\eta - s))]\, \mathrm{d}s, \tag{18b}$$

where

$$\lambda_{m1}^4 = \left[\frac{(m\pi)^2}{\beta^2} - \alpha^2\right]^2, \quad \lambda_{m2}^4 = \left[\frac{(m\pi)^2}{\beta^2} + \alpha^2\right]^2. \tag{19}$$

When $\alpha > m\pi/\beta$:

$$W_m(\eta) = A_m \sin(\lambda_{m1}\eta) + B_m \cos(\lambda_{m1}\eta) + C_m \sinh(\lambda_{m2}\eta) + D_m \cosh(\lambda_{m2}\eta) + \tilde{W}_m(\eta) \tag{20a}$$

$$\tilde{W}_m(\eta) = \frac{b^4}{D\alpha^2\lambda_{m1}\lambda_{m2}} \int_0^\eta F_m(s)[\lambda_{m1}\sinh(\lambda_{m2}(\eta - s)) - \lambda_{m2}\sin(\lambda_{m1}(\eta - s))]\,\mathrm{d}s. \tag{20b}$$

In Eqs. (18a) and (20a), the first four terms with unknown constants A_m, B_m, C_m and D_m are the homogeneous solutions while $\tilde{W}_m(\eta)$ is the special solution.

Assuming a positive integer L, when $m < L$, $\alpha > m\pi/\beta$ and when $m \geqslant L$, $\alpha < m\pi/\beta$, the modal shape $W(\xi, \eta)$ in Eq. (15) can be expressed as

$$\begin{aligned} W(\xi,\eta) = {} & \sum_{m=1}^{L-1} \sin(m\pi\xi)\Bigg\{ A_m \sin(\lambda_{m1}\eta) + B_m \cos(\lambda_{m1}\eta) + C_m \sinh(\lambda_{m2}\eta) + D_m \cosh(\lambda_{m2}\eta) \\ & + \frac{b^4}{D\alpha^2\lambda_{m1}\lambda_{m2}} \int_0^\eta F_m(s)[\lambda_{m1}\sinh(\lambda_{m2}(\eta - s)) - \lambda_{m2}\sin(\lambda_{m1}(\eta - s))]\,\mathrm{d}s \Bigg\} \\ & + \sum_{m=L}^{\infty} \sin(m\pi\xi)\Bigg\{ A_m \sinh(\lambda_{m1}\eta) + B_m \cosh(\lambda_{m1}\eta) + C_m \sinh(\lambda_{m2}\eta) + D_m \cosh(\lambda_{m2}\eta) \\ & + \frac{b^4}{D\alpha^2\lambda_{m1}\lambda_{m2}} \int_0^\eta F_m(s)[\lambda_{m1}\sinh(\lambda_{m2}(\eta - s)) - \lambda_{m2}\sinh(\lambda_{m1}(\eta - s))]\,\mathrm{d}s \Bigg\}. \end{aligned} \tag{21}$$

Substituting Eq. (9) into Eq. (16) leads to:

$$\begin{aligned} F_m(\eta) = {} & \frac{1}{ab}\sum_{i=1}^{n} P_i \sin(m\pi\xi_i)\delta(\eta - \eta_i) + \frac{1}{a^2 b}\sum_{i=1}^{n} M_{xi} m\pi \cos(m\pi\xi_i)\delta(\eta - \eta_i) \\ & + \frac{1}{ab^2}\sum_{i=1}^{n} M_{yi} \sin(m\pi\eta_i)\delta'(\xi - \xi_i). \end{aligned} \tag{22}$$

Substituting Eq. (22) into Eq. (21) gives

$$\begin{aligned} W(\xi,\eta) = {} & \sum_{m=1}^{L-1} \sin(m\pi\xi)\Bigg\{ A_m \sin(\lambda_{m1}\eta) + B_m \cos(\lambda_{m1}\eta) + C_m \sinh(\lambda_{m2}\eta) + D_m \cosh(\lambda_{m2}\eta) \\ & + \frac{b^2}{\beta D\alpha^2\lambda_{m1}\lambda_{m2}} \sum_{i=1}^{n} P_i \sin(m\pi\xi_i)\big[\lambda_{m1}\sinh(\lambda_{m2}(\eta - \eta_i)) - \lambda_{m2}\sin(\lambda_{m1}(\eta - \eta_i))\big] H(\eta - \eta_i) \\ & - \frac{bm\pi}{\beta^2 D\alpha^2\lambda_{m1}\lambda_{m2}} \sum_{i=1}^{n} M_{xi} \cos(m\pi\xi_i)\big[\lambda_{m1}\sinh(\lambda_{m2}(\eta - \eta_i)) - \lambda_{m2}\sin(\lambda_{m1}(\eta - \eta_i))\big] H(\eta - \eta_i) \\ & - \frac{b}{\beta D\alpha^2} \sum_{i=1}^{n} M_{yi} \sin(m\pi\xi_i)\big[\cosh(\lambda_{m2}(\eta - \eta_i)) - \cos(\lambda_{m1}(\eta - \eta_i))\big] H(\eta - \eta_i) \Bigg\} \\ & + \sum_{m=L}^{\infty} \sin(m\pi\xi)\Bigg\{ A_m \sinh(\lambda_{m1}\eta) + B_m \cosh(\lambda_{m1}\eta) + C_m \sinh(\lambda_{m2}\eta) + D_m \cosh(\lambda_{m2}\eta) \\ & + \frac{b^2}{\beta D\alpha^2\lambda_{m1}\lambda_{m2}} \sum_{i=1}^{n} P_i \sin(m\pi\xi_i)\big[\lambda_{m1}\sinh(\lambda_{m2}(\eta - \eta_i)) - \lambda_{m2}\sinh(\lambda_{m1}(\eta - \eta_i))\big] H(\eta - \eta_i) \end{aligned}$$

$$-\frac{bm\pi}{\beta^2 D\alpha^2\lambda_{m1}\lambda_{m2}}\sum_{i=1}^{n} M_{xi}\cos(m\pi\xi_i)\left[\lambda_{m1}\sinh(\lambda_{m2}(\eta-\eta_i))-\lambda_{m2}\sinh(\lambda_{m1}(\eta-\eta_i))\right]H(\eta-\eta_i)$$
$$-\frac{b}{\beta D\alpha^2}\sum_{i=1}^{n} M_{yi}\sin(m\pi\xi_i)\left[\cosh(\lambda_{m2}(\eta-\eta_i))-\cosh(\lambda_{m1}(\eta-\eta_i))\right]H(\eta-\eta_i)\Bigg\}, \tag{23}$$

where $H(\eta-\eta_i)=\begin{cases}0 & \eta<\eta_i,\\ 1 & \eta\geqslant\eta_i,\end{cases}$ is the Heaviside function.

The solutions of longitudinal and transverse vibrations of the ith column can be obtained as follows:

$$U_i(\zeta_i)=\Psi_{1i}\sin(s_i\zeta_i)+\Psi_{2i}\cos(s_i\zeta_i), \tag{24a}$$

$$V_{xi}(\zeta_i)=\Phi_{xi1}\sin(r_{xi}\zeta_i)+\Phi_{xi2}\cos(r_{xi}\zeta_i)+\Phi_{xi3}\sinh(r_{xi}\zeta_i)+\Phi_{xi4}\cosh(r_{xi}\zeta_i), \tag{24b}$$

$$V_{yi}(\zeta_i)=\Phi_{yi1}\sin(r_{yi}\zeta_i)+\Phi_{yi2}\cos(r_{yi}\zeta_i)+\Phi_{yi3}\sinh(r_{yi}\zeta_i)+\Phi_{yi4}\cosh(r_{yi}\zeta_i), \tag{24c}$$

where $s_i=\sqrt{\rho_i/E_i}\omega l_i$ and $r_{xi}=\sqrt[4]{\frac{\rho_i A_i}{E_i I_{xi}}\omega^2 l_i^4}$, $r_{yi}=\sqrt[4]{\frac{\rho_i A_i}{E_i I_{yi}}\omega^2 l_i^4}$. Ψ_{1i}, $\Psi_{2i}(i=1,2,\ldots,n)$ and Φ_{xij}, Φ_{yij} $(j=1,2,3,4,\ i=1,2,\ldots,n)$ are the unknown constants.

5. Unknown coefficients

Substituting Eq. (23) into Eq. (12), the unknown constants A_m, B_m, C_m and D_m can be determined. As an example, for the plate simply supported at $\eta=0$ and $\eta=1$,

$$B_m=D_m=0; \tag{25}$$

when $m<L$:

$$A_m=\frac{b^2}{\beta D\alpha^2\sin\lambda_{m1}}\left\{\frac{1}{\lambda_{m1}}\sum_{i=1}^{n}P_i\sin(m\pi\xi_i)\sin(\lambda_{m1}(1-\eta_i))\right.$$
$$-\frac{m\pi}{\beta\lambda_{m1}}\sum_{i=1}^{n}\frac{M_{xi}}{b}\cos(m\pi\xi_i)\sin(\lambda_{m1}(1-\eta_i))$$
$$\left.-\sum_{i=1}^{n}\frac{M_{yi}}{b}\sin(m\pi\xi_i)\cos(\lambda_{m1}(1-\eta_i))\right\}, \tag{26a}$$

$$C_m=-\frac{b^2}{\beta D\alpha^2\sinh\lambda_{m2}}\left\{\frac{1}{\lambda_{m2}}\sum_{i=1}^{n}P_i\sin(m\pi\xi_i)\sinh(\lambda_{m2}(1-\eta_i))\right.$$
$$-\frac{m\pi}{\beta\lambda_{m2}}\sum_{i=1}^{n}\frac{M_{xi}}{b}\cos(m\pi\xi_i)\sinh(\lambda_{m2}(1-\eta_i))$$
$$\left.-\sum_{i=1}^{n}\frac{M_{yi}}{b}\sin(m\pi\xi_i)\cosh(\lambda_{m2}(1-\eta_i))\right\}, \tag{26b}$$

when $m\geqslant L$:

$$A_m=\frac{b^2}{\beta D\alpha^2\sinh\lambda_{m1}}\left\{\frac{1}{\lambda_{m1}}\sum_{i=1}^{n}P_i\sin(m\pi\xi_i)\sinh(\lambda_{m1}(1-\eta_i))\right.$$
$$-\frac{m\pi}{\beta\lambda_{m1}}\sum_{i=1}^{n}\frac{M_{xi}}{b}\cos(m\pi\xi_i)\sinh(\lambda_{m1}(1-\eta_i))$$
$$\left.-\sum_{i=1}^{n}\frac{M_{yi}}{b}\sin(m\pi\xi_i)\cosh(\lambda_{m1}(1-\eta_i))\right\}, \tag{27a}$$

$$C_m = -\frac{b^2}{\beta D\alpha^2 \sinh\lambda_{m2}}\left\{\frac{1}{\lambda_{m2}}\sum_{i=1}^{n} P_i \sin(m\pi\xi_i)\sinh(\lambda_{m2}(1-\eta_i)) - \frac{m\pi}{\beta\lambda_{m2}}\sum_{i=1}^{n}\frac{M_{xi}}{b}\cos(m\pi\xi_i)\sinh(\lambda_{m2}(1-\eta_i)) - \sum_{i=1}^{n}\frac{M_{yi}}{b}\sin(m\pi\xi_i)\cosh(\lambda_{m2}(1-\eta_i))\right\}. \tag{27b}$$

Substituting Eqs. (26) and (27) into Eq. (23) gives

$$\begin{aligned}
W(\xi,\eta) = {} & \frac{b^2}{\beta D\alpha^2}\sum_{m=1}^{L-1}\sin(m\pi\xi)\left\{\sum_{i=1}^{n} P_i \sin(m\pi\xi_i)\left\{\frac{1}{\lambda_{m1}\sin\lambda_{m1}}\sin(\lambda_{m1}(1-\eta_i))\sin(\lambda_{m1}\eta)\right.\right. \\
& -\frac{1}{\lambda_{m2}\sinh\lambda_{m2}}\sinh(\lambda_{m2}(1-\eta_i))\sinh(\lambda_{m2}\eta)+\frac{1}{\lambda_{m1}\lambda_{m2}}[\lambda_{m1}\sinh(\lambda_{m2}(\eta-\eta_i)) \\
& \left.-\lambda_{m2}\sin(\lambda_{m1}(\eta-\eta_i))]H(\eta-\eta_i)\right\} - \frac{m\pi}{\beta}\sum_{i=1}^{n}\frac{M_{xi}}{b}\cos(m\pi\xi_i) \\
& \times\left\{\frac{1}{\lambda_{m1}\sin\lambda_{m1}}\sin(\lambda_{m1}(1-\eta_i))\sin(\lambda_{m1}\eta)-\frac{1}{\lambda_{m2}\sinh\lambda_{m2}}\sinh(\lambda_{m2}(1-\eta_i))\sinh(\lambda_{m2}\eta)\right. \\
& \left.+\frac{1}{\lambda_{m1}\lambda_{m2}}[\lambda_{m1}\sinh(\lambda_{m2}(\eta-\eta_i))-\lambda_{m2}\sin(\lambda_{m1}(\eta-\eta_i))]H(\eta-\eta_i)\right\} - \sum_{i=1}^{n}\frac{M_{yi}}{b}\sin(m\pi\xi_i) \\
& \times\left\{\frac{1}{\sin\lambda_{m1}}\cos(\lambda_{m1}(1-\eta_i))\sin(\lambda_{m1}\eta)-\frac{1}{\sinh\lambda_{m2}}\cosh(\lambda_{m2}(1-\eta_i))\sinh(\lambda_{m2}\eta)\right. \\
& \left.\left.+[\cosh(\lambda_{m2}(\eta-\eta_i))-\cos(\lambda_{m1}(\eta-\eta_i))]H(\eta-\eta_i)\right\}\right\} \\
& +\frac{b^2}{\beta D\alpha^2}\sum_{m=L}^{\infty}\sin(m\pi\xi)\left\{\sum_{i=1}^{n} P_i \sin(m\pi\xi_i)\left\{\frac{1}{\lambda_{m1}\sinh\lambda_{m1}}\sinh(\lambda_{m1}(1-\eta_i))\sinh(\lambda_{m1}\eta)\right.\right. \\
& -\frac{1}{\lambda_{m2}\sinh\lambda_{m2}}\sinh(\lambda_{m2}(1-\eta_i))\sinh(\lambda_{m2}\eta)+\frac{1}{\lambda_{m1}\lambda_{m2}}[\lambda_{m1}\sinh(\lambda_{m2}(\eta-\eta_i)) \\
& \left.-\lambda_{m2}\sinh(\lambda_{m1}(\eta-\eta_i))]H(\eta-\eta_i)\right\} - \frac{m\pi}{\beta}\sum_{i=1}^{n}\frac{M_{xi}}{b}\cos(m\pi\xi_i) \\
& \times\left\{\frac{1}{\lambda_{m1}\sinh\lambda_{m1}}\sinh(\lambda_{m1}(1-\eta_i))\sinh(\lambda_{m1}\eta)-\frac{1}{\lambda_{m2}\sinh\lambda_{m2}}\sinh(\lambda_{m2}(1-\eta_i))\sinh(\lambda_{m2}\eta)\right. \\
& \left.+\frac{1}{\lambda_{m1}\lambda_{m2}}[\lambda_{m1}\sinh(\lambda_{m2}(\eta-\eta_i))-\lambda_{m2}\sinh(\lambda_{m1}(\eta-\eta_i))]H(\eta-\eta_i)\right\} \\
& -\sum_{i=1}^{n}\frac{M_{yi}}{b}\sin(m\pi\xi_i)\left\{\frac{1}{\sinh\lambda_{m1}}\cosh(\lambda_{m1}(1-\eta_i))\sinh(\lambda_{m1}\eta)-\frac{1}{\sinh\lambda_{m2}}\cosh(\lambda_{m2}(1-\eta_i))\sinh(\lambda_{m2}\eta)\right. \\
& \left.\left.+[\cosh(\lambda_{m2}(\eta-\eta_i))-\cosh(\lambda_{m1}(\eta-\eta_i))]H(\eta-\eta_i)\right\}\right\}.
\end{aligned} \tag{28}$$

Substituting the three formulae in Eq. (24) into the appropriate expressions in Eq. (13), the unknown constants Ψ_{1i}, $\Psi_{2i}(i=1,2,\ldots,n)$ and Φ_{xij}, $\Phi_{yij}(j=1,2,3,4,\ i=1,2,\ldots,n)$ can be uniquely determined. For example, for columns clamped at $\zeta_i=0$ $(i=1,2,\ldots,n)$, there are

$$V_{xi}(\zeta_i) = \frac{M_{xi}l_i^2}{2E_iI_{xi}r_{xi}^2}\left\{G_{xi1}[\sin(r_{xi}\zeta_i)-\sinh(r_{xi}\zeta_i)] - G_{xi2}[\cos(r_{xi}\zeta_i)-\cosh(r_{xi}\zeta_i)]\right\}, \tag{29a}$$

$$V_{yi}(\zeta_i) = \frac{M_{yi}l_i^2}{2E_iI_{yi}r_{yi}^2}\left\{G_{yi1}\left[\sin(r_{yi}\zeta_i) - \sinh(r_{yi}\zeta_i)\right] - G_{yi2}\left[\cos(r_{yi}\zeta_i) - \cosh(r_{yi}\zeta_i)\right]\right\}, \tag{29b}$$

$$U_i(\zeta_i) = \frac{P_i l_i}{E_i A_i s_i \cos s_i}\sin(s_i\zeta_i), \tag{29c}$$

in which,

$$G_{xi1} = \frac{\cos r_{xi} - \cosh r_{xi}}{\sin r_{xi}\cosh r_{xi} - \cos r_{xi}\sinh r_{xi}}, \tag{30a}$$

$$G_{xi2} = \frac{\sin r_{xi} - \sinh r_{xi}}{\sin r_{xi}\cosh r_{xi} - \cos r_{xi}\sinh r_{xi}}, \tag{30b}$$

$$G_{yi1} = \frac{\cos r_{yi} - \cosh r_{yi}}{\sin r_{yi}\cosh r_{yi} - \cos r_{yi}\sinh r_{yi}}, \tag{30c}$$

$$G_{yi2} = \frac{\sin r_{yi} - \sinh r_{yi}}{\sin r_{yi}\cosh r_{yi} - \cos r_{yi}\sinh r_{yi}}. \tag{30d}$$

6. Eigenfrequency equation

The unknown forces P_i and moments M_{xi}, M_{yi} $(i = 1, 2, \ldots, n)$ can be determined from the compatibility of displacements and rotations between the plate and the columns. Substituting Eqs. (28) and (29) into Eq. (14) produces a group of homogeneous equations for M_{xi}, M_{yi} and P_i $(i = 1, 2, \ldots, n)$ as follows

$$\begin{bmatrix} [\mathbf{A^1}] & [\mathbf{B^1}] & [\mathbf{C^1}] \\ [\mathbf{A^2}] & [\mathbf{B^2}] & [\mathbf{C^2}] \\ [\mathbf{A^3}] & [\mathbf{B^3}] & [\mathbf{C^3}] \end{bmatrix} \begin{Bmatrix} \{\mathbf{P}\} \\ \{\overline{\mathbf{M}}_\mathbf{x}\} \\ \{\overline{\mathbf{M}}_\mathbf{y}\} \end{Bmatrix} = \begin{Bmatrix} \{\mathbf{0}\} \\ \{\mathbf{0}\} \\ \{\mathbf{0}\} \end{Bmatrix}, \tag{31}$$

where

$$[\mathbf{A^k}] = \begin{bmatrix} A_{11}^k & A_{12}^k & \cdots & A_{1n}^k \\ A_{12}^k & A_{22}^k & \cdots & A_{2n}^k \\ \vdots & \vdots & \ddots & \vdots \\ A_{n1}^k & A_{n2}^k & \cdots & A_{nn}^k \end{bmatrix}, \quad [\mathbf{B^k}] = \begin{bmatrix} B_{11}^k & B_{12}^k & \cdots & B_{1n}^k \\ B_{12}^k & B_{22}^k & \cdots & B_{2n}^k \\ \vdots & \vdots & \ddots & \vdots \\ B_{n1}^k & B_{n2}^k & \cdots & B_{nn}^k \end{bmatrix},$$

$$[\mathbf{C^k}] = \begin{bmatrix} C_{11}^k & C_{12}^k & \cdots & C_{1n}^k \\ C_{12}^k & C_{22}^k & \cdots & C_{2n}^k \\ \vdots & \vdots & \ddots & \vdots \\ C_{n1}^k & C_{n2}^k & \cdots & C_{nn}^k \end{bmatrix}, \quad k = 1, 2, 3, \tag{32a}$$

$$\{\mathbf{P}\} = \begin{Bmatrix} P_1 \\ P_2 \\ \vdots \\ P_n \end{Bmatrix}, \quad \{\overline{\mathbf{M}}_\mathbf{x}\} = \begin{Bmatrix} M_{x1}/b \\ M_{x2}/b \\ \vdots \\ M_{xn}/b \end{Bmatrix}, \quad \{\overline{\mathbf{M}}_\mathbf{y}\} = \begin{Bmatrix} M_{y1}/b \\ M_{y2}/b \\ \vdots \\ M_{yn}/b \end{Bmatrix}. \tag{32b}$$

The elements in the sub-matrices (32a) are given in the appendix in which,

$$\Delta_i = \frac{\tan s_i}{s_i}, \tag{33a}$$

$$\Gamma_{xi} = [G_{xi1}(\cos r_{xi} - \cosh r_{xi}) + G_{xi2}(\sin r_{xi} + \sinh r_{xi})]/(2r_{xi}), \tag{33b}$$

$$\Gamma_{yi} = [G_{yi1}(\cos r_{yi} - \cosh r_{yi}) + G_{yi2}(\sin r_{yi} + \sinh r_{yi})]/(2r_{yi}), \tag{33c}$$

$$\tau_i = \frac{Dl_i}{E_i A_i b^2}, \quad \sigma_{xi} = \frac{Dl_i}{E_i I_{xi}}, \quad \sigma_{yi} = \frac{Dl_i}{E_i I_{yi}}, \quad \delta_{ij} = \begin{cases} 1 & i = j, \\ 0 & i \neq j. \end{cases} \tag{34}$$

Here, Δ_i, Γ_{xi} and Γ_{yi} are referred to as the dynamic stiffness coefficients of the ith column in the longitudinal and two rotational directions, respectively. τ_i, σ_{xi} and σ_{yi} are referred to as dimensionless stiffnesses of the ith column in these directions, respectively. In order to obtain the non-zero solutions for P_i, $\overline{M}_{xi}$, $\overline{M}_{yi} (i = 1, 2, \ldots, n)$, the determinant of coefficient matrix in Eq. (31) should be zero, i.e.

$$\begin{vmatrix} [\mathbf{A^1}] & [\mathbf{B^1}] & [\mathbf{C^1}] \\ [\mathbf{A^2}] & [\mathbf{B^2}] & [\mathbf{C^2}] \\ [\mathbf{A^3}] & [\mathbf{B^3}] & [\mathbf{C^3}] \end{vmatrix} = 0. \tag{35}$$

Eq. (35) is nonlinear in respect of the eigenfrequency ω which can be determined using the searching root method. In the present analysis, the common bisection method is used to obtain the roots. If a non-real root appears, the value of the determinant in Eq. (35) would be infinite rather than zero. A small step length such as 10^{-3} in the search is used to ensure that no roots are missed. Substituting the known ω into Eq. (31) yields the associated coefficient vector containing $\{P\}$, $\{\overline{M}_x\}$ and $\{\overline{M}_y\}$. Then, substituting these results into Eq. (28) gives the vibration modes of the plate–column system. Substituting Eq. (29) into Eq. (14), it can be noted that if $W(\xi, \eta) = \partial W/\partial \xi = \partial W/\partial \eta = 0$ at the connection point $(\xi = \xi_j, \eta = \eta_j)$ of the plate–column system, then $P_j = M_{xj} = M_{yj} = 0$. This means that the vibrations of the plate and the jth column are independent because no rotation occurs at the connection point. Giving dimensionless stiffnesses τ_i, σ_{xi} and σ_{yi} extreme values, several special cases can be obtained. For example, taking $\tau_j = \sigma_{xj} = \sigma_{yj} = 0$ provides a fixed point-support at (x_j, y_j), taking $\sigma_{xj} = \sigma_{yj} = \infty$ means ignoring the effect of rotational constraints of the jth column to the plate and the column acts as a vertical bar, and taking $\tau_j = 0$, $\sigma_{xj} = \sigma_{yj} = \infty$ means a pinned point-support at (x_j, y_j).

It is a common approximation in engineering to model each column as three springs without masses. One spring is vertical, which constrains the vertical displacement of the plate. The other two springs are rotational, which constrain the rotations of the plate in two concerned directions, respectively. The static displacements of the ith column under P_i, M_{xi} and M_{yi} can be easily obtained as follows:

$$U_i(\zeta_i) = \frac{P_i l_i}{E_i A_i}\zeta_i, \quad V_{xi} = \frac{M_{xi} l_i^2}{4E_{xi} I_{xi}}(\zeta_i^3 - \zeta_i^2), \quad V_{yi} = \frac{M_{yi} l_i^2}{4E_{yi} I_{yi}}(\zeta_i^3 - \zeta_i^2). \tag{36}$$

In such a case, the dynamic stiffness coefficients Δ_i, Γ_{xi} and Γ_{yi} defined in Eq. (33) reduce to

$$\Delta_i = 1, \quad \Gamma_{xi} = \Gamma_{yi} = 1/4. \tag{37}$$

7. Numerical studies

In order to identify the effect of columns on floor vibrations, the numerical analyses of fully simply supported rectangular plates with one internal column support are undertaken. In all the

calculation, the first 200 terms of each series were used to guarantee that the results are at least accurate to 10^{-4} for all cases except for the fully simply supported plates with one column near to or at its centre where an improved approach, as given in the following sub-section, is used. In the following study, it is assumed that the columns and the plate are made of the same material and the Poission's ratio, v, is 0.2.

7.1. Improved convergence

It should be mentioned that the convergence rate of Eq. (35) depends on the positions of the columns. The closer the columns to the centre of the plate, the lower the convergence rate. However, an improved approach can be used for this case. Consider the fact that for a fully simply supported plate, interchanging the variables ξ and η in Eq. (27) should produce a valid solution. Hence, Eq. (27) can be rewritten in an identical form to M_{xi} and M_{yi}. In order to save the space, the detailed process is omitted but the three sub-matrices for M_{xi} in the appendix should be replaced by the following formulae:

$$\begin{aligned} B_{ij}^1 = & -\sum_{m=1}^{L-1} \sin(m\pi\eta_i)\sin(m\pi\eta_i)\left\{\frac{1}{\sin\tilde{\lambda}_{m1}}\cos(\tilde{\lambda}_{m1}(1-\xi_j))\sin(\tilde{\lambda}_{m1}\xi_j)\right. \\ & -\frac{1}{\sinh\tilde{\lambda}_{m2}}\cosh(\tilde{\lambda}_{m2}(1-\xi_i))\sinh(\tilde{\lambda}_{m2}\xi_j)+[\cosh(\tilde{\lambda}_{m2}(\xi_j-\xi_i)) \\ & \left.-\cos(\tilde{\lambda}_{m1}(\xi_j-\xi_i))]H(\xi_j-\xi_i)\right\}-\sum_{m=L}^{\infty}\sin(m\pi\eta_i)\sin(m\pi\eta_j) \\ & \left\{\frac{1}{\sinh\tilde{\lambda}_{m1}}\cosh(\tilde{\lambda}_{m1}(1-\xi_i))\sinh(\tilde{\lambda}_{m1}\xi_j)-\frac{1}{\sinh\tilde{\lambda}_{m2}}\cosh(\tilde{\lambda}_{m2}(1-\xi_i))\sinh(\tilde{\lambda}_{m2}\xi_j)\right. \\ & \left.+[\cosh(\tilde{\lambda}_{m2}(\xi_j-\xi_i))-\cosh(\tilde{\lambda}_{m1}(\xi_j-\xi_i))]H(\xi_j-\xi_i)\right\} \end{aligned} \tag{38a}$$

$$\begin{aligned} B_{ij}^2 = & \sum_{m=1}^{L-1}\sin(m\pi\eta_i)\sin(m\pi\eta_j)\left\{\frac{\tilde{\lambda}_{m1}}{\sin\tilde{\lambda}_{m1}}\cos(\tilde{\lambda}_{m1}(1-\xi_i))\cos(\tilde{\lambda}_{m1}\xi_j)\right. \\ & -\frac{\tilde{\lambda}_{m2}}{\sinh\tilde{\lambda}_{m2}}\cosh(\tilde{\lambda}_{m2}(1-\xi_i))\cosh(\tilde{\lambda}_{m2}\xi_j) \\ & \left.+[\tilde{\lambda}_{m2}\sinh(\tilde{\lambda}_{m2}(\xi_j-\xi_i))+\tilde{\lambda}_{m1}\sin(\tilde{\lambda}_{m1}(\xi_j-\xi_i))]H(\xi_j-\xi_i)\right\} \\ & +\sum_{m=L}^{\infty}\sin(m\pi\eta_i)\sin(m\pi\eta_j)\left\{\frac{\tilde{\lambda}_{m1}}{\sinh\tilde{\lambda}_{m1}}\cosh(\tilde{\lambda}_{m1}(1-\xi_i))\cosh(\tilde{\lambda}_{m1}\xi_j)\right. \\ & -\frac{\tilde{\lambda}_{m2}}{\sinh\tilde{\lambda}_{m2}}\cosh(\tilde{\lambda}_{m2}(1-\xi_i))\cosh(\tilde{\lambda}_{m2}\xi_j)+[\tilde{\lambda}_{m2}\sinh(\tilde{\lambda}_{m2}(\xi_j-\xi_i)) \\ & \left.-\tilde{\lambda}_{m1}\sinh(\tilde{\lambda}_{m1}(\xi_j-\xi_i))]H(\xi_j-\xi_i)\right\}-\beta\alpha^2\Gamma_{xi}\sigma_{xi}\delta_{ij}, \end{aligned} \tag{38b}$$

$$\begin{aligned} B_{ij}^3 = & \sum_{m=1}^{L-1} m\pi\sin(m\pi\eta_i)\cos(m\pi\eta_j)\left\{\frac{1}{\sin\tilde{\lambda}_{m1}}\cos(\tilde{\lambda}_{m1}(1-\xi_i))\sin(\tilde{\lambda}_{m1}\xi_j)\right. \\ & \left.-\frac{1}{\sinh\tilde{\lambda}_{m2}}\cosh(\tilde{\lambda}_{m2}(1-\xi_i))\sinh(\tilde{\lambda}_{m2}\xi_j)+[\cosh(\tilde{\lambda}_{m2}(\xi_j-\xi_i))\right. \end{aligned}$$

$$-\cos(\tilde{\lambda}_{m1}(\xi_j-\xi_i))]H(\xi_j-\xi_i)\Big\}+\sum_{m=L}^{\infty} m\pi\sin(m\pi\eta_i)\cos(m\pi\eta_j)$$
$$\Big\{\frac{1}{\sinh\tilde{\lambda}_{m1}}\cosh(\tilde{\lambda}_{m1}(1-\xi_i))\sinh(\tilde{\lambda}_{m1}\xi_j)-\frac{1}{\sinh\tilde{\lambda}_{m2}}\cosh(\tilde{\lambda}_{m2}(1-\xi_i))\sinh(\tilde{\lambda}_{m2}\xi_j)$$
$$+[\cosh(\tilde{\lambda}_{m2}(\xi_j-\xi_i))-\cosh(\tilde{\lambda}_{m1}(\xi_j-\xi_i))]H(\xi_j-\xi_i)\Big\} \tag{38c}$$

in which

$$\tilde{\lambda}_{m1}^4=\beta^4\left[(m\pi)^2-\alpha^2\right]^2,\quad \tilde{\lambda}_{m2}^4=\beta^4\left[(m\pi)^2+\alpha^2\right]^2. \tag{39}$$

Using the above formulae, more rapid convergence can be achieved in the numerical calculation.

7.2. Comparative study

Plates with two different aspect ratios and supported by a column with two different square cross-sectional sizes are, respectively, analysed using the proposed method. One plate is square and has the sides of $a=b=16\,\text{m}$, the other plate is rectangular and has the sides of $a=21\,\text{m}$ and $b=14\,\text{m}$. Both plates have the same thickness of $h=0.25\,\text{m}$. Two column cross-sections are considered with $a_c=b_c=0.4\,\text{m}$ and $a_c=b_c=0.3\,\text{m}$ respectively. The sides of the column cross-sections are parallel to the sides of the plates. The column has a constant length of $l=5\,\text{m}$. An elastic modulus of $E=30\times10^9\,\text{N/m}^2$ and a material density of $\rho=2400\,\text{kg/m}^3$ are used in the calculation. Two different support positions of the column are considered. One is at $(\xi_1=0.5,\eta_1=0.5)$ and the other is at $(\xi_1=0.375,\eta_1=0.25)$. Two extreme cases are also considered when the column is replaced by a pinned vertical support or a fixed point support. The first six natural frequencies of the two plates, each including eight cases, are given in Table 1. The first mode for the simply supported square plate with a column (cross-sectional sizes $a_c=b_c=0.3\,\text{m}$) at its centre is given in Fig. 2, in which the column only provides the longitudinal restraint to the plate. The first mode for the simply supported square plate with a fixed point-support at $\xi_1=0.375$, $\eta_1=0.25$ is given in Fig. 3, in which the deflection and rotations of the plate at the support point are zero. The first mode for the simply supported square plate with a column (cross-section size $a_c=b_c=0.3\,\text{m}$) at $\xi_1=0.375$, $\eta_1=0.25$ is given in Fig. 4. In such a case, the column provides both the longitudinal and the rotational restraints to the plate. The FE solutions resulting from the commercial software package LUSAS [11] are used to check the present solutions. The thin shell elements QSI4 (4 nodes for each element and 6 degrees of freedom (dof) on each node) are used to model the plate and the thick beam elements BMS3 (3 nodes for each element and 5 dof on each node) are used to model the column in the calculations. Different mesh divisions are taken, including 8×8, 16×16, 32×32 and 64×64 elements for the plate, and 5 and 10 elements for the column. The first six natural frequencies of the FE solutions from the different mesh divisions are almost the same. For comparison, the FE solutions in the case of 32×32 elements for the plate and 10 elements for the column are listed in Table 1. It can be seen from Table 1 that:

- The present results closely agree with the FE solutions for all cases.
- For the square plate with a column support at its centre, the fourth and fifth frequencies are constants in all the cases. For the rectangular plate with a column at its centre, the fourth frequency is also a constant in all the cases.
- The natural frequencies of the plates supported by columns are not always larger than those of the plates with pinned point-supports at the corresponding locations.

It is well known that if a bare plate has a duplicate natural frequency, the corresponding modes are degenerated: an arbitrary linear combination of these two modes has the same natural frequency. Therefore, it is always possible to find a coefficient to let the combined mode be zero at any selected

Table 1
Comparison of the first six natural frequencies (Hz) f_i ($i = 1, 2, \ldots, 6$) of a plate with one internal column support

ξ_1, η_1	a_c, b_c	f_1	f_2	f_3	f_4	f_5	f_6
Square plate, $a = b = 16\,\text{m}$, $h = 0.25\,\text{m}$							
0.5, 0.5	0.3 m, 0.3 m	8.041	8.073	8.073	12.784	15.979	20.796
		(8.040)	(8.072)	(8.072)	(12.773)	(15.963)	(20.770)
	0.4 m, 0.4 m	8.195	8.195	8.241	12.784	15.979	20.844
		(8.203)	(8.203)	(8.241)	(12.773)	(15.963)	(20.821)
	Fixed point-support	8.519	8.570	8.570	12.784	15.979	20.995
		(8.519)	(8.696)	(8.696)	(12.773)	(15.963)	(21.020)
	Pinned point-support	7.989	7.989	8.519	12.784	15.979	20.774
		(7.986)	(7.986)	(8.519)	(12.773)	(15.963)	(20.746)
0.375, 0.25	0.3 m, 0.3 m	4.583	8.017	10.888	14.479	16.015	18.509
		(4.583)	(8.014)	(10.883)	(14.468)	(16.000)	(18.498)
	0.4 m, 0.4 m	4.639	8.056	10.988	14.638	16.075	18.727
		(4.640)	(8.056)	(10.984)	(14.634)	(16.064)	(18.709)
	Fixed point-support	4.753	8.172	11.152	14.996	16.262	19.008
		(4.777)	(8.206)	(11.165)	(15.071)	(16.308)	(18.992)
	Pinned point-support	4.637	7.989	11.064	14.606	15.979	18.993
		(4.637)	(7.986)	(11.057)	(14.594)	(15.963)	(18.974)
Rectangular plate, $a = 21\,\text{m}$, $b = 14\,\text{m}$, $h = 0.25\,\text{m}$							
0.5, 0.5	0.3 m, 0.3 m	5.857	6.638	9.358	12.059	14.041	16.736
		(5.856)	(6.637)	(9.353)	(12.049)	(14.034)	(16.720)
	0.4 m, 0.4 m	5.938	6.739	9.479	12.059	14.314	16.807
		(5.947)	(6.738)	(9.481)	(12.049)	(14.307)	(16.795)
	Fixed point-support	6.181	6.874	9.865	12.059	14.698	17.066
		(6.273)	(6.873)	(9.955)	(12.049)	(14.690)	(17.121)
	Pinned point-support	5.797	6.874	9.276	12.059	14.698	16.696
		(5.795)	(6.873)	(9.270)	(12.049)	(14.690)	(16.679)
0.375, 0.25	0.3 m, 0.3 m	4.272	6.565	10.294	11.030	14.093	16.774
		(4.272)	(6.563)	(10.288)	(11.024)	(14.083)	(16.757)
	0.4 m, 0.4 m	4.318	6.629	10.321	11.102	14.241	16.820
		(4.319)	(6.630)	(10.317)	(11.100)	(14.233)	(16.808)
	Fixed point-support	4.411	6.776	10.383	11.277	14.468	16.974
		(4.429)	(6.807)	(10.393)	(11.326)	(14.474)	(17.020)
	Pinned point-support	4.317	6.607	10.295	11.071	14.393	16.748
		(4.317)	(6.605)	(10.289)	(11.064)	(14.382)	(16.730)

Data in parentheses come from FE solutions.

location of the plate. When a square plate has a column support at its centre, the first-order derivatives of the double symmetric modes in the two perpendicular directions are always equal to zero at the centre of the plate. In such a case, a combination of the double symmetric duplicate modes can give a new mode which not only has zero displacement but also zero first-order derivatives at the centre of the plate in the two directions. Taking a fully simply supported square plate as an example, the $(1, 3)$ mode $\sin(\pi\xi)\sin(3\pi\eta)$ and the $(3, 1)$ mode $\sin(3\pi\xi)\sin(\pi\eta)$ are both double symmetric modes with the same natural frequency. Therefore, whether or not there is a column support at the centre of the plate, a frequency $f = 5\pi/b^2\sqrt{D/\rho h}\,\text{Hz}$ for the double symmetric mode can always be obtained. The fifth natural frequency of the square plate with a central column support just corresponds to such a mode. Moreover, the double antisymmetric modes of the bare plate always satisfy the conditions of zero-deflection and zero-rotations at the centre in the ξ and η directions. The fourth frequency of the square and rectangular plates with a central column support corresponds to the first double antisymmetric mode of the bare plate.

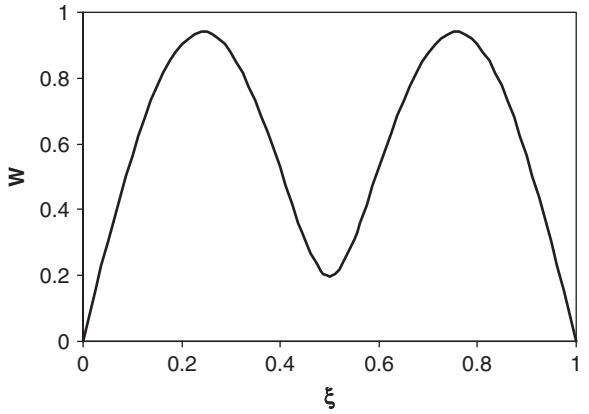

Fig. 2. The first mode of the square plate with a column support at its centre, i.e., the cutaway view when $\eta = 0.5$.

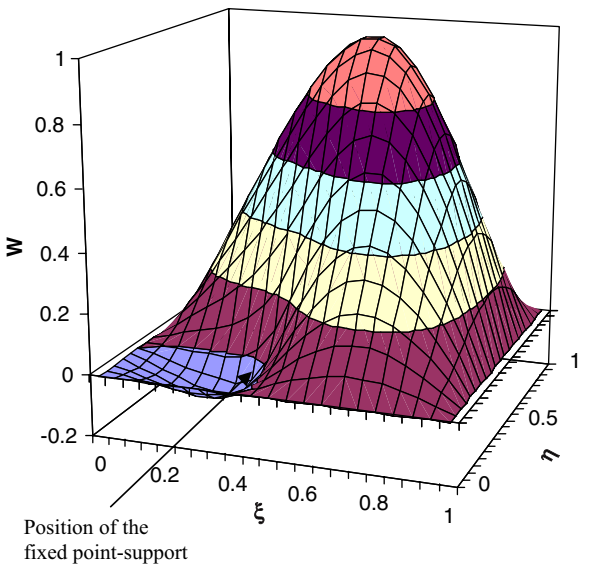

Fig. 3. The first mode of the square plate with a fixed point-support at $\xi_1 = 0.375$, $\eta_1 = 0.25$.

7.3. *Effect of column sizes*

Consider a fully simply supported square plate with aspect ratio $a/b = 1$ and thickness ratio $h/b = 0.02$ with a square cross-section column support at the centre of the plate. In such a case, the vibration modes of the plate–column system can be classified into double symmetric, symmetric–antisymmetric, antisymmetric–symmetric and double antisymmetric modes. For the double symmetric modes, only the longitudinal stiffness of the column contributes to the vibration of the system while for the symmetric–antisymmetric and antisymmetric–symmetric modes, only the rotational stiffness of the column contributes to the vibration. Neither the longitudinal stiffness nor the rotational stiffness contributes to the double antisymmetric vibration. Hence it is possible to investigate separately the effect of column size on the natural frequencies of a plate–column system. A non-dimensional

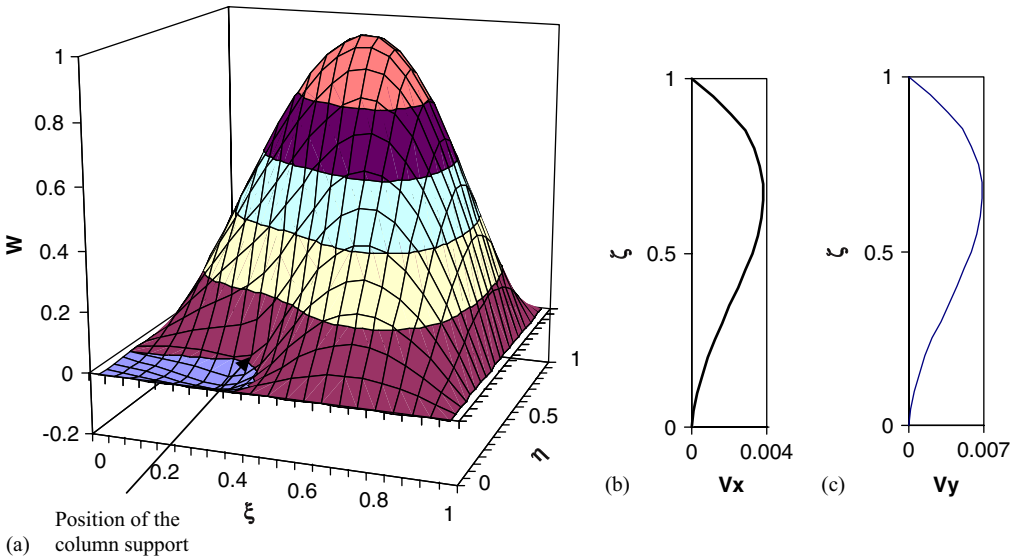

Fig. 4. The first mode of the square plate with a column support at $\xi_1 = 0.375$, $\eta_1 = 0.25$, (a) the mode of the plate, (b) the flexural mode of the column in the ξ–ζ plane, (c) the flexural mode of the column in the η–ζ plane.

frequency parameter, defined as $\lambda = \omega b^2\sqrt{\rho h/D}$, is introduced. Table 2 gives λ_i^{ss} $(i = 1, 3, 4)$ for the double symmetric modes and λ_i^{as} $(i = 1, 2, 3)$ for the antisymmetric-symmetric modes or λ_i^{sa} $(i = 1, 2, 3)$ for the symmetric-antisymmetric modes. It is obvious that the frequencies of the antisymmetric-symmetric modes are the same as those of the symmetric-antisymmetric modes due to the double symmetry of the structure. The second double symmetric mode $\lambda_2^{ss} = 98.696$ and all the double antisymmetric modes are not included in the table, because they are always constants and independent of the size of the column.

Changing the sizes of the column will result in different frequency parameters. In the present study, four column length ratios $l/b = 0.4, 0.5, 0.6, 0.7$ and four cross-sectional size ratios $a_c/h = 1.5, 2, 3, 4$ are considered respectively. It can be seen from Table 2 that:

- The sensitivity of the frequency parameters depends on both l/b and a_c/h. The frequency parameters of antisymmetric–symmetric modes (or symmetric–antisymmetric modes) are more sensitive to the sizes of the column than those of double symmetric modes.
- The increase of column length ratio and/or decrease of the cross-sectional size ratio will result in the monotonic decrease of frequency parameters.
- When the column becomes thicker, i.e. l/b reduces and/or a_c/h increases, the results become closer to those of a slab with a fixed point-support.
- A column support at the centre of a plate can greatly increase the natural frequency of the first double symmetric mode of the plate ($\lambda = 47.478$-52.62 versus $\lambda = 19.739$).

7.4. Effect of column models

In engineering practice, different column models have been used. This section examines the effect of column models on the frequency parameters of the plate–column system. Four different column models are considered as follows:

- The column is treated as a pinned point-support.
- The column is treated as a fixed point-support.

Table 2
The size effect of the column on the frequency parameter $\lambda = \alpha^2 = \omega b^2\sqrt{\rho h/D}$ of a plate-column structure with $a/b = 1.0$ and $h/b = 0.02$

l/b	a_c/h	λ_1^{ss}	λ_3^{ss}	λ_4^{ss}	λ_1^{as}, λ_1^{sa}	λ_2^{as}, λ_2^{sa}	λ_3^{as}, λ_3^{sa}
0.4	1.5	49.523	137.38	196.59	50.373	128.46	165.06
	2	50.816	141.26	200.65	51.383	128.97	169.08
	3	51.798	144.23	204.28	52.475	129.48	171.67
	4	52.154	145.29	205.70	52.775	129.61	172.24
0.5	1.5	48.818	135.14	194.35	50.128	116.05	129.79
	2	50.385	139.84	198.90	51.119	127.81	140.98
	3	51.594	143.56	203.31	52.362	129.37	170.12
	4	52.037	144.91	205.11	52.736	129.59	172.07
0.6	1.5	48.134	132.94	192.27	49.816	82.823	128.89
	2	49.960	138.36	197.09	50.814	99.328	129.53
	3	51.392	142.84	202.22	52.236	127.80	134.06
	4	51.920	144.50	204.44	52.691	129.53	175.64
0.7	1.5	47.478	130.80	190.33	49.100	62.382	128.62
	2	49.541	136.83	195.22	50.320	74.816	129.20
	3	51.188	142.06	200.97	52.069	98.191	129.70
	4	51.803	144.05	203.64	52.638	125.15	130.36
Fixed point-support		52.620	146.67	207.64	52.934	129.68	172.50
Pinned point-support		52.620	146.67	207.64	49.348	128.30	167.78
No column		19.739	98.696	177.65	49.348	128.30	167.78

- The column is modelled as a bar, which only provides vertical stiffness (the bar model).
- The column is modelled as three springs representing the actual stiffnesses of the column but without considering the mass of the column (the spring model).

The comparison of results from the above four approximate models to those from the exact model are given in Table 3. A square plate $a/b = 1$ with thickness ratio $h/b = 0.025$ is studied with a column of circular cross-section of diameter d placed at the centre of the plate. Three different column length ratios $l/b = 0.4$, 0.5, 0.6and two different cross-sectional size ratios $d/h = 1.5$, 3.0 are considered respectively. It is found that:

- With the increase of the column length ratio and/or the decrease of the cross-sectional size ratio, the lower order modes are dominated by the column vibration. However, such a mode cannot be predicted by using any of the approximate column models. For examples, for a column having the sizes of $d/h = 1.5$, $l/b = 0.5$ or 0.6 and for a column having the sizes of $d/h = 3$, $l/b = 0.6$, the second antisymmetric-symmetric mode cannot be found using the approximate column models.
- The fixed point-supported column model in most cases leads to the largest errors of the four approximate column models.
- The bar and spring models are better than the fixed and pinned point-support models, and provide good approximations to the exact solutions in most cases.

8. Conclusions

This paper presents an exact solution for the study of free vibration of a thin rectangular plate with two opposite edges simply supported and internal column supports. The governing differential equations of the free vibration of the plate–column system are solved directly.

Table 3
Frequency parameter $\lambda = \alpha^2 = \omega b^2\sqrt{\rho h/D}$ of a plate-column structure with $a/b = 1.0$ and $h/b = 0.025$

d/h	l/b	λ_1^{ss}	λ_3^{ss}	λ_4^{ss}	λ_1^{as}, λ_1^{sa}	λ_2^{as}, λ_2^{sa}	λ_3^{as}, λ_3^{sa}
1.5	0.4	47.909	132.55	192.25	50.147	128.22	156.35
		(47.909)	(132.55)	(192.25)	(49.348)	(128.30)	(167.78)
		[47.930]	[133.16]	[193.26]	[50.224]	[128.64]	[168.82]
	0.5	46.896	129.49	189.71	49.909	103.57	129.09
		(46.896)	(129.49)	(189.71)	(49.348)	*	(128.30)
		[46.948]	[130.52]	[191.32]	[50.082]	*	[128.58]
	0.6	45.942	126.63	187.50	49.547	73.465	128.70
		(45.942)	(126.63)	(187.50)	(49.348)	*	(128.30)
		[46.011]	[128.16]	[189.73]	[49.976]	*	[128.55]
3	0.4	51.323	142.72	202.24	52.333	129.41	171.32
		(51.323)	(142.72)	(202.24)	(49.348)	(128.30)	(167.78)
		[51.328]	[142.97]	[202.83]	[52.354]	[129.46]	[171.66]
	0.5	51.005	141.59	200.60	52.191	129.20	162.68
		(51.005)	(141.59)	(200.60)	(49.348)	(128.30)	(167.78)
		[51.024]	[142.04]	[201.76]	[52.228]	[129.40]	[170.50]
	0.6	50.687	140.34	198.69	52.019	116.02	130.10
		(50.687)	(140.34)	(198.69)	(49.348)	*	(128.30)
		[50.721]	[141.15]	[200.77]	[52.119]	*	[129.38]
Fixed point-support		52.620	146.67	207.64	52.934	129.68	172.50
Pinned point-support		52.620	146.67	207.64	49.348	128.30	167.78

The data in parentheses are the results for the column modelled as a bar and the data in square brackets are the results for the column modelled as springs without mass.

The correctness and the accuracy of the present method are demonstrated by the comparison of the results obtained from the proposed method and from FE method. Thus, the solutions provided can be used as benchmarks for further investigations and for other approximate methods. In order to understand better the effect of a column in floor vibration, the following has been investigated:

- The effect of column parameters, including the length, the cross-section size and the location of the column.

It has been shown that increasing the length of the column and/or decreasing the cross-sectional size of the column will decrease the natural frequencies of the structure. A column support at the centre of a plate can greatly increase the natural frequency of the first double symmetric mode of the plate.

- The effect of column models, including the pinned point-support model, the fixed point-support model, the bar model and the spring model.

It is found that the fixed point-support model always overestimates the natural frequencies of the structure and produces the largest errors in all the four approximate models. With the increase of column length and the decrease of cross-sectional size, the modes dominated by the column vibration become the low-order ones, which cannot be predicted by any of the approximate column models. In this situation, the actual column model should be taken.

Acknowledgements

The work reported in this paper has been conducted as part of the project "Prediction of floor vibration induced by walking loads and verification using available measurements" funded by the UK Engineering and Physical Sciences Research Council (EPSRC Grant No GR/S74089), which is

gratefully acknowledged. Thanks are given to Dr Emad El-Dardiry for carrying out the finite-element calculations.

Appendix

The elements in Eq. (32a) are given as follows:

$$
\begin{aligned}
A_{ij}^{1} = & \sum_{m=1}^{L-1} \sin(m\pi\xi_i)\sin(m\pi\xi_j)\left\{\frac{1}{\lambda_{m1}\sin\lambda_{m1}}\sin(\lambda_{m1}(1-\eta_i))\sin(\lambda_{m1}\eta_j)\right. \\
& -\frac{1}{\lambda_{m2}\sinh\lambda_{m2}}\sinh(\lambda_{m2}(1-\eta_i))\sinh(\lambda_{m2}\eta_j) \\
& \left.+\frac{1}{\lambda_{m1}\lambda_{m2}}[\lambda_{m1}\sinh(\lambda_{m2}(\eta_j-\eta_i))-\lambda_{m2}\sin(\lambda_{m1}(\eta_j-\eta_i))]H(\eta_j-\eta_i)\right\} \\
& +\sum_{m=L}^{\infty} \sin(m\pi\xi_i)\sin(m\pi\xi_j)\left\{\frac{1}{\lambda_{m1}\sinh\lambda_{m1}}\sinh(\lambda_{m1}(1-\eta_i))\sinh(\lambda_{m1}\eta_j)\right. \\
& -\frac{1}{\lambda_{m2}\sinh\lambda_{m2}}\sinh(\lambda_{m2}(1-\eta_i))\sinh(\lambda_{m2}\eta_j) \\
& +\frac{1}{\lambda_{m1}\lambda_{m2}}[\lambda_{m1}\sinh(\lambda_{m2}(\eta_j-\eta_i)) \\
& \left.-\lambda_{m2}\sinh(\lambda_{m1}(\eta_j-\eta_i))]H(\eta_j-\eta_i)\right\}+\beta\alpha^2\tau_i\Delta_i\delta_{ij},
\end{aligned}
$$

$$
\begin{aligned}
B_{ij}^{1} = & -\sum_{m=1}^{L-1} \frac{m\pi}{\beta}\cos(m\pi\xi_i)\sin(m\pi\xi_j)\left\{\frac{1}{\lambda_{m1}\sin\lambda_{m1}}\sin(\lambda_{m1}(1-\eta_i))\sin(\lambda_{m1}\eta_j)\right. \\
& -\frac{1}{\lambda_{m2}\sinh\lambda_{m2}}\sinh(\lambda_{m2}(1-\eta_i))\sinh(\lambda_{m2}\eta_j) \\
& \left.+\frac{1}{\lambda_{m1}\lambda_{m2}}[\lambda_{m1}\sinh(\lambda_{m2}(\eta_j-\eta_i))-\lambda_{m2}\sin(\lambda_{m1}(\eta_j-\eta_i))]H(\eta_j-\eta_i)\right\} \\
& -\sum_{m=L}^{\infty} \frac{m\pi}{\beta}\cos(m\pi\xi_i)\sin(m\pi\xi_j)\left\{\frac{1}{\lambda_{m1}\sinh\lambda_{m1}}\sinh(\lambda_{m1}(1-\eta_i))\sinh(\lambda_{m1}\eta_j)\right. \\
& -\frac{1}{\lambda_{m2}\sinh\lambda_{m2}}\sinh(\lambda_{m2}(1-\eta_i))\sinh(\lambda_{m2}\eta_j) \\
& \left.+\frac{1}{\lambda_{m1}\lambda_{m2}}[\lambda_{m1}\sinh(\lambda_{m2}(\eta_j-\eta_i))-\lambda_{m2}\sinh(\lambda_{m1}(\eta_j-\eta_i))]H(\eta_j-\eta_i)\right\},
\end{aligned}
$$

$$
\begin{aligned}
C_{ij}^{1} = & -\sum_{m=1}^{L-1} \sin(m\pi\xi_i)\sin(m\pi\xi_j)\left\{\frac{1}{\sin\lambda_{m1}}\cos(\lambda_{m1}(1-\eta_i))\sin(\lambda_{m1}\eta_j)\right. \\
& -\frac{1}{\sinh\lambda_{m2}}\cosh(\lambda_{m2}(1-\eta_i))\sinh(\lambda_{m2}\eta_j)+[\cosh(\lambda_{m2}(\eta_j-\eta_i)) \\
& \left.-\cos(\lambda_{m1}(\eta_j-\eta_i))]H(\eta_j-\eta_i)\right\}-\sum_{m=L}^{\infty} \sin(m\pi\xi_i)\sin(m\pi\xi_j) \\
& \times\left\{\frac{1}{\sinh\lambda_{m1}}\cosh(\lambda_{m1}(1-\eta_i))\sinh(\lambda_{m1}\eta_j)-\frac{1}{\sinh\lambda_{m2}}\cosh(\lambda_{m2}(1-\eta_i))\sinh(\lambda_{m2}\eta_j)\right. \\
& \left.+[\cosh(\lambda_{m2}(\eta_j-\eta_i))-\cosh(\lambda_{m1}(\eta_j-\eta_i))]H(\eta_j-\eta_i)\right\},
\end{aligned}
$$

$$
\begin{aligned}
A_{ij}^2 = & -\sum_{m=1}^{L-1} m\pi \sin(m\pi\xi_i)\cos(m\pi\xi_j)\left\{\frac{1}{\lambda_{m1}\sin\lambda_{m1}}\sin(\lambda_{m1}(1-\eta_i))\sin(\lambda_{m1}\eta_j)\right.\\
& -\frac{1}{\lambda_{m2}\sinh\lambda_{m2}}\sinh(\lambda_{m2}(1-\eta_i))\sinh(\lambda_{m2}\eta_j)\\
& \left.+\frac{1}{\lambda_{m1}\lambda_{m2}}[\lambda_{m1}\sinh(\lambda_{m2}(\eta_j-\eta_i))-\lambda_{m2}\sin(\lambda_{m1}(\eta_j-\eta_i))]H(\eta_j-\eta_i)\right\}\\
& -\sum_{m=L}^{\infty} m\pi \sin(m\pi\xi_i)\cos(m\pi\xi_j)\left\{\frac{1}{\lambda_{m1}\sinh\lambda_{m1}}\sinh(\lambda_{m1}(1-\eta_i))\sinh(\lambda_{m1}\eta_j)\right.\\
& -\frac{1}{\lambda_{m2}\sinh\lambda_{m2}}\sinh(\lambda_{m2}(1-\eta_i))\sinh(\lambda_{m2}\eta_j)\\
& \left.+\frac{1}{\lambda_{m1}\lambda_{m2}}[\lambda_{m1}\sinh(\lambda_{m2}(\eta_j-\eta_i))-\lambda_{m2}\sinh(\lambda_{m1}(\eta_j-\eta_i))]H(\eta_j-\eta_i)\right\},
\end{aligned}
$$

$$
\begin{aligned}
B_{ij}^2 = & \sum_{m=1}^{L-1}\frac{(m\pi)^2}{\beta}\cos(m\pi\xi_i)\cos(m\pi\xi_j)\left\{\frac{1}{\lambda_{m1}\sin\lambda_{m1}}\sin(\lambda_{m1}(1-\eta_i))\sin(\lambda_{m1}\eta_j)\right.\\
& -\frac{1}{\lambda_{m2}\sinh\lambda_{m2}}\sinh(\lambda_{m2}(1-\eta_i))\sinh(\lambda_{m2}\eta_j)\\
& \left.+\frac{1}{\lambda_{m1}\lambda_{m2}}[\lambda_{m1}\sinh(\lambda_{m2}(\eta_j-\eta_i))-\lambda_{m2}\sin(\lambda_{m1}(\eta_j-\eta_i))]H(\eta_j-\eta_i)\right\}\\
& +\sum_{m=L}^{\infty}\frac{(m\pi)^2}{\beta}\cos(m\pi\xi_i)\cos(m\pi\xi_j)\left\{\frac{1}{\lambda_{m1}\sinh\lambda_{m1}}\sinh(\lambda_{m1}(1-\eta_i))\sinh(\lambda_{m1}\eta_j)\right.\\
& -\frac{1}{\lambda_{m2}\sinh\lambda_{m2}}\sinh(\lambda_{m2}(1-\eta_i))\sinh(\lambda_{m2}\eta_j)\\
& \left.+\frac{1}{\lambda_{m1}\lambda_{m2}}[\lambda_{m1}\sinh(\lambda_{m2}(\eta_j-\eta_i))-\lambda_{m2}\sinh(\lambda_{m1}(\eta_j-\eta_i))]H(\eta_j-\eta_i)\right\}\\
& -\beta^2\alpha^2\Gamma_{xi}\sigma_{xi}\delta_{ij},
\end{aligned}
$$

$$
\begin{aligned}
C_{ij}^2 = & \sum_{m=1}^{L-1} m\pi \sin(m\pi\xi_i)\cos(m\pi\xi_j)\left\{\frac{1}{\sin\lambda_{m1}}\cos(\lambda_{m1}(1-\eta_i))\sin(\lambda_{m1}\eta_j)\right.\\
& -\frac{1}{\sinh\lambda_{m2}}\cosh(\lambda_{m2}(1-\eta_i))\sinh(\lambda_{m2}\eta_j)+[\cosh(\lambda_{m2}(\eta_j-\eta_i))\\
& \left.-\cos(\lambda_{m1}(\eta_j-\eta_i))]H(\eta_j-\eta_i)\right\}+\sum_{m=L}^{\infty} m\pi \sin(m\pi\xi_i)\cos(m\pi\xi_j)\\
& \left\{\frac{1}{\sinh\lambda_{m1}}\cosh(\lambda_{m1}(1-\eta_i))\sinh(\lambda_{m1}\eta_j)-\frac{1}{\sinh\lambda_{m2}}\cosh(\lambda_{m2}(1-\eta_i))\sinh(\lambda_{m2}\eta_j)\right.\\
& \left.+[\cosh(\lambda_{m2}(\eta_j-\eta_i))-\cosh(\lambda_{m1}(\eta_j-\eta_i))]H(\eta_j-\eta_i)\right\},
\end{aligned}
$$

$$
\begin{aligned}
A_{ij}^3 = & -\sum_{m=1}^{L-1}\sin(m\pi\xi_i)\sin(m\pi\xi_j)\left\{\frac{1}{\sin\lambda_{m1}}\sin(\lambda_{m1}(1-\eta_i))\cos(\lambda_{m1}\eta_j)\right.\\
& \left.-\frac{1}{\sinh\lambda_{m2}}\sinh(\lambda_{m2}(1-\eta_i))\cosh(\lambda_{m2}\eta_j)\right.
\end{aligned}
$$

$$+[\cosh(\lambda_{m2}(\eta_j-\eta_i))-\cos(\lambda_{m1}(\eta_j-\eta_i))]H(\eta_j-\eta_i)\Big\}$$
$$-\sum_{m=L}^{\infty}\sin(m\pi\xi_i)\sin(m\pi\xi_j)\Big\{\frac{1}{\sinh\lambda_{m1}}\sinh(\lambda_{m1}(1-\eta_i))\cosh(\lambda_{m1}\eta_j)$$
$$-\frac{1}{\sinh\lambda_{m2}}\sinh(\lambda_{m2}(1-\eta_i))\cosh(\lambda_{m2}\eta_j)+[\cosh(\lambda_{m2}(\eta_j-\eta_i))$$
$$-\cosh(\lambda_{m1}(\eta_j-\eta_i))]H(\eta_j-\eta_i)\Big\},$$

$$B_{ij}^3=\sum_{m=1}^{L-1}\frac{m\pi}{\beta}\cos(m\pi\xi_i)\sin(m\pi\xi_j)\Big\{\frac{1}{\sin\lambda_{m1}}\sin(\lambda_{m1}(1-\eta_i))\cos(\lambda_{m1}\eta_j)$$
$$-\frac{1}{\sinh\lambda_{m2}}\sinh(\lambda_{m2}(1-\eta_i))\cosh(\lambda_{m2}\eta_j)+[\cosh(\lambda_{m2}(\eta_j-\eta_i))$$
$$-\cos(\lambda_{m1}(\eta_j-\eta_i))]H(\eta_j-\eta_i)\Big\}+\sum_{m=L}^{\infty}\frac{m\pi}{\beta}\cos(m\pi\xi_i)\sin(m\pi\xi_j)$$
$$\Big\{\frac{1}{\sinh\lambda_{m1}}\sinh(\lambda_{m1}(1-\eta_i))\cosh(\lambda_{m1}\eta_j)-\frac{1}{\sinh\lambda_{m2}}\sinh(\lambda_{m2}(1-\eta_i))\cosh(\lambda_{m2}\eta_j)$$
$$+[\cosh(\lambda_{m2}(\eta_j-\eta_i))-\cosh(\lambda_{m1}(\eta_j-\eta_i))]H(\eta_j-\eta_i)\Big\},$$

$$C_{ij}^3=\sum_{m=1}^{L-1}\sin(m\pi\xi_i)\sin(m\pi\xi_j)\Big\{\frac{\lambda_{m1}}{\sin\lambda_{m1}}\cos(\lambda_{m1}(1-\eta_i))\cos(\lambda_{m1}\eta_j)$$
$$-\frac{\lambda_{m2}}{\sinh\lambda_{m2}}\cosh(\lambda_{m2}(1-\eta_i))\cosh(\lambda_{m2}\eta_j)$$
$$+[\lambda_{m2}\sinh(\lambda_{m2}(\eta_j-\eta_i))+\lambda_{m1}\sin(\lambda_{m1}(\eta_j-\eta_i))]H(\eta_j-\eta_i)\Big\}$$
$$+\sum_{m=L}^{\infty}\sin(m\pi\xi_i)\sin(m\pi\xi_j)\Big\{\frac{\lambda_{m1}}{\sinh\lambda_{m1}}\cosh(\lambda_{m1}(1-\eta_i))\cosh(\lambda_{m1}\eta_j)$$
$$-\frac{\lambda_{m2}}{\sinh\lambda_{m2}}\cosh(\lambda_{m2}(1-\eta_i))\cosh(\lambda_{m2}\eta_j)+[\lambda_{m2}\sinh(\lambda_{m2}(\eta_j-\eta_i))$$
$$-\lambda_{m1}\sinh(\lambda_{m1}(\eta_j-\eta_i))]H(\eta_j-\eta_i)\Big\}-\beta\alpha^2\Gamma_{yi}\sigma_{yi}\delta_{ij}.$$

References

[1] B.R. Ellis, T. Ji, Dynamic testing and numerical modelling of the Cardington steel framed building from construction to completion, *Structural Engineering* 74 (1996) 186–192.

[2] S.C. Fan, Y.K. Cheung, Flexural free vibrations of rectangular plates with complex support conditions, *Journal of Sound and Vibration* 93 (1984) 81–94.

[3] C.S. Kim, S.M. Dickinson, The flexural vibration of rectangular plates with point supports, *Journal of Sound and Vibration* 117 (1987) 249–261.

[4] D. Zhou, Vibrations of point-supported rectangular plates with variable thickness using a set of static tapered beam functions, *International Journal of Mechanical Sciences* 44 (2002) 149–164.

[5] Y.K. Cheung, D. Zhou, The free vibrations of rectangular composite plates with point-supports using static beam functions, *Composite Structures* 44 (1999) 145–154.

[6] D. Zhou, Y.K. Cheung, J. Kong, Free vibration of thick, layered rectangular plates with point supports by finite layer method, *International Journal of Solids and Structures* 37 (2000) 1483–1499.

[7] K.M. Liew, S. Kitipornchai, M.K. Lim, Vibration of Mindlin plates on point supports using constraint functions, *ASCE Journal of Engineering Mechanics* 120 (1994) 499–513.
[8] L.A. Bergman, J.K. Hall, G.G.G. Lueschen, D.M. McFarland, Dynamic Green's functions for Levy plates, *Journal of Sound and Vibration* 162 (1993) 281–310.
[9] M. Petyt, W.H. Mirza, Vibration of column-supported floor slabs, *Journal of Sound and Vibration* 21 (1972) 355–364.
[10] E. El-Dardiry, E. Wanhyuni, T. Ji, B.R. Ellis, Improving FE models of a long-span flat concrete floor using natural frequency measurements, *Computers & Structure* 80 (2002) 2145–2156.
[11] FEA Ltd., LUSAS User Manual, Kingeston-upon-Thames, 1993.